

Immunosuppressive Small Molecule Discovered by Structure-Based Virtual Screening for Inhibitors of Protein–Protein Interactions**

Tim Geppert, Stefanie Bauer, Jan A. Hiss, Elea Conrad, Michael Reutlinger, Petra Schneider, Martin Weisel, Bernhard Pfeiffer, Karl-Heinz Altmann, Zoe Waibler, and Gisbert Schneider*

Type I interferons (referred to as IFN- α and IFN- β) are pro-inflammatory cytokines that confer cellular resistance to viral infections.^[1] They constitute a first line of defense against pathogens and critically contribute to the initial survival of the host until the onset of adaptive immunity.^[2] Plasmacytoid dendritic cells (pDCs) are the main type I IFN producers.^[3] All type I IFNs bind one common receptor (IFNAR), thereby initiating a positive feedback loop leading to elevated IFN levels.^[4] There is evidence that chronically activated pDCs produce IFN- α in response to stimulation of toll-like receptors (TLRs), possibly contributing to the pathogenesis of systemic lupus erythematosus, a severe autoimmune disorder.^[5] Similar immunotoxic symptoms can occur during IFN treatment of chronic hepatitis and autoimmune type 1 diabetes.^[6,7]

Here, we report the identification of a nonpeptidic, low-molecular-weight inhibitor of the interaction between IFN- α and IFNAR by means of virtual compound screening. We present a computer-based molecular design strategy, which we applied to finding druglike inhibitors of protein–protein interactions (PPIs)^[8] with minimal experimental effort. The resulting lead compound significantly reduces IFN- α production by murine pDCs in vitro. NMR and surface plasmon resonance (SPR) experiments confirm the direct interaction of the inhibitor with IFN- α . Our findings demonstrate that computer-based models can provide relevant hypotheses

about contact sites in macromolecular complexes and modulation by druglike compounds. We anticipate this proof-of-concept study to foster drug-discovery projects aiming at the therapeutic suppression of high IFN titers, and provide a broadly applicable technology for the rapid identification of PPI inhibitors.

NMR solution structures of human IFN- α alone (PDB ID: 1itt^[9] model 16) and in complex with the receptor's ectodomain, IFNAR2-EC (PDB ID: 2hym^[10] model 6), were taken from the Protein Data Bank (PDB)^[11] (Figure 1 A). We selected representative low-energy conformations with the lowest average root-mean-square deviation (rmsd) to the

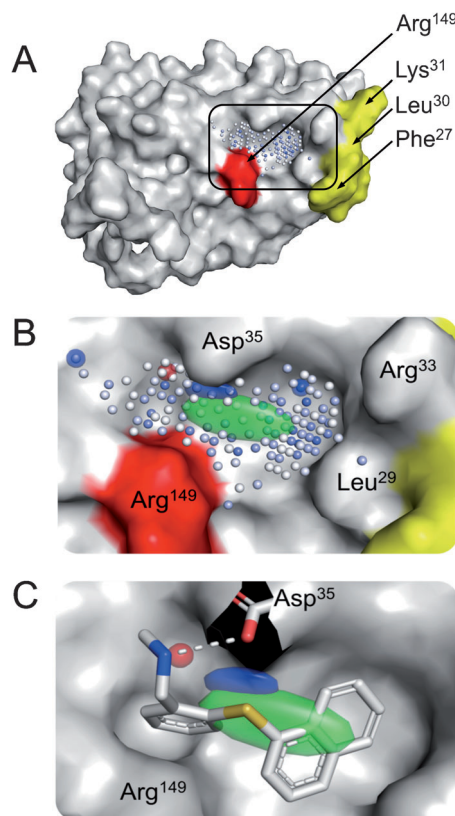


Figure 1. Interface of IFN- α with its receptor, IFNAR. A) The target pocket on the surface of IFN- α , represented by blue dots. Predicted interface residues ("hot spots") are colored in red (highest score) and yellow (medium score). B) "Virtual ligand" pharmacophore model inside the binding pocket (green: lipophilic center, blue: hydrogen-bond donor, red: hydrogen-bond acceptor). C) Overlay of the docking pose of compound 1 and the virtual-ligand model. A potential hydrogen-bond donor–acceptor interaction between Asp³⁵ and compound 1 is highlighted by a dotted line.

[*] T. Geppert, Dr. J. A. Hiss, M. Reutlinger, Dr. P. Schneider, B. Pfeiffer, Prof. Dr. K.-H. Altmann, Prof. Dr. G. Schneider^[†]
Eidgenössische Technische Hochschule (ETH) Zürich
Department of Chemistry and Applied Biosciences
Wolfgang-Pauli-Strasse 10, 8093 Zürich (Switzerland)
E-mail: gisbert.schneider@pharma.ethz.ch

S. Bauer, E. Conrad, Priv.-Doz. Dr. Z. Waibler^[†]
Junior Research Group "Novel Vaccination Strategies and Early Immune Responses", Paul-Ehrlich-Institut
63225 Langen (Germany)

Dr. M. Weisel
Goethe-Universität Frankfurt, Institut für Organische Chemie und Chemische Biologie, Beilstein-Stiftungsprofessur, Frankfurt (Germany)

[†] These authors contributed equally to this work.

[**] We thank Kay-Martin Hanschmann and Peter Volkers for statistical analyses, and Gerd Sutter for providing MVA. Martin Löwer implemented the VirtualLigand software. The Chemical Computing Group Inc. kindly provided a research license for MOE. This research was supported by the Swiss National Science Foundation (grant 205321-134783), the OPO-Foundation Zurich (G.S.), and the Deutsche Forschungsgemeinschaft (grant WA 2873/1-1 to Z.W.).

Supporting information for this article is available on the WWW under <http://dx.doi.org/10.1002/anie.201105901>.

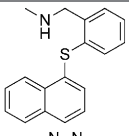
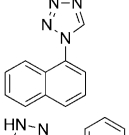
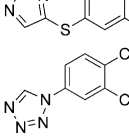
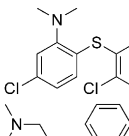
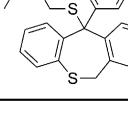
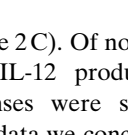
NMR models deposited in the data files (rmsd = (2.6 ± 0.4) Å for IFN- α , rmsd = (1.0 ± 0.1) Å for IFNAR2-EC). The IFN- α contact surface to IFNAR2-EC covers an area of 801 Å². Since the contact areas of protein–protein and protein–drug interactions typically overlap,^[12] and to avoid local conformations induced by IFN–IFNAR interaction,^[13] we decided to identify the most promising ligand-binding site in the unbound IFN- α structure. The average rmsd between bound and unbound IFN- α is 1.14 Å. The receptor interface is defined by two disconnected sequence fragments (His⁷–Gln⁴⁶, Pro¹³⁷–Glu¹⁶⁵), for which the corresponding rmsd is 1.5 Å. This greater value indicates a larger conformational change in this part of the protein upon receptor binding than for the remainder of the structure.

We then searched for a potential ligand-binding pocket on the IFN- α interface surface by using our software tool PocketPicker^[14] for cavity extraction, and the iPred^[15] method for the identification of surface “hot spots” in protein–protein interaction sites. The software detected a total of 19 candidate pockets, three of which reside within the binding cleft of the (IFN- α)–(IFNAR2-EC2) complex. Interface analysis resulted in six hot-spot residues, four of which (Phe²⁷, Leu³⁰, Lys³¹, Arg¹⁴⁹) surround a pocket with a volume of approximately 155 Å³ (Figure 1 A). The predictions are in perfect agreement with previous mutation studies analyzing the interaction of human IFNAR with IFN- α .^[16,17] Notably, these biochemical experiments suggested additional residues to be important for the interaction, whereas iPred predictions are confined to the binding groove and clearly highlight an essential interaction core.

Based on the protein model, we generated a permissive (“fuzzy”) pharmacophore model inside the extracted pocket using our VirtualLigand^[18] approach. Potential ligand–receptor interaction sites were computed as Gaussian densities (Figure 1 B) for the virtual screening of a collection of 556 763 commercially available compounds. From the top-ranking 100, six candidates were manually selected and automatically docked into the IFN- α pocket using GOLD v5.0.1 software^[19] (Table 1, Figure 1 C). Positive docking scores (GoldScore function) indicate favorable binding of all six compounds, with compound **1** ranking highest.

To test the ability of the six candidate compounds to inhibit IFN- α responses, murine bone-marrow-derived, Flt3-L-differentiated pDC cultures (BM-pDCs) were infected with modified *Vaccinia* virus ankara (MVA), which is known to induce IFN- α responses by these cells,^[20] and co-treated with candidate compounds. Compound **1** was able to completely inhibit MVA-induced IFN- α responses by BM-pDCs (IC₅₀ = 2–8 μM), whereas compounds **2–4** did not block MVA-induced IFN responses (Figure 2 A,B). Compounds **5** and **6** turned out to be insoluble in the test buffer and thus could not be used for experiments. To test the specificity of the IFN- α inhibition by compound **1**, we measured interleukin (IL)-12 (IL-12p70 and p40) concentrations in the supernatant of MVA-infected and compound-treated BM-pDCs. IL-12 production after MVA infection should not be affected by IFN–IFNAR PPI. We observed reduced IL-12 production at high compound concentrations only (Figure 2 B), which might be related to the cellular toxicity of compound **1** at high dosages

Table 1: Compounds suggested by virtual screening and tested for inhibition of IFN- α response in vitro ($n = 4$).

No.	Structure	Inhibition (%±standard deviation)	GoldScore
1		99 ± 2	54
2		14 ± 35	35
3		12 ± 25	43
4		1 ± 33	34
5		insoluble in DMSO	50
6		insoluble in DMSO	53

(Figure 2 C). Of note, at intermediate compound dosages the total IL-12 production was unaffected, whereas IFN- α responses were significantly reduced (Figure 2 B). From these data we conclude that compound **1** specifically inhibits IFN- α responses upon MVA infection of BM-pDCs.

To study whether treatment with compound **1** primarily inhibited MVA-induced IFN- α responses or whether IFN- α responses induced by other stimuli were also impaired, BM-pDC cultures were treated with three stimuli known to induce robust IFN- α responses by BM-pDCs: TLR9 ligand CpG2216,^[21] MDA5/TLR3 ligand poly(I:C),^[22] and infection with vesicular stomatitis virus (VSV) variant M2.^[23] Indeed, compound **1** inhibited the IFN- α responses that were elicited after treatment with CpG2216, stimulation with poly(I:C), and infection with VSV-M2, whereas the total IL-12 production was notably less affected under those conditions (Figure 2 D).

We used saturation-transfer difference (STD) NMR spectroscopy^[24] to investigate whether compound **1** binds to human IFN- α . ¹H NMR reference spectra were recorded for compound **1** and IFN- α separately (Figure 3 A,B), as well as the off-resonance reference (Figure 3 C) and STD spectrum (Figure 3 D) for the mixture of compound **1** with IFN- α . Saturation transfer can be seen best in the aromatic range of the spectrum and from the methyl signal of compound **1**. Signals from the aromatic protons of compound **1** (7.0–8.5 ppm) and the N-methyl group (2.7 ppm) are clearly visible in the STD spectrum, which suggests the direct binding of compound **1** to IFN- α . To verify the specific binding of compound **1** to IFN- α , we repeated the experiment with methyl- β -D-glucopyranoside as a presumed nonbinder. From the corresponding off-resonance reference (Figure 3 E) and

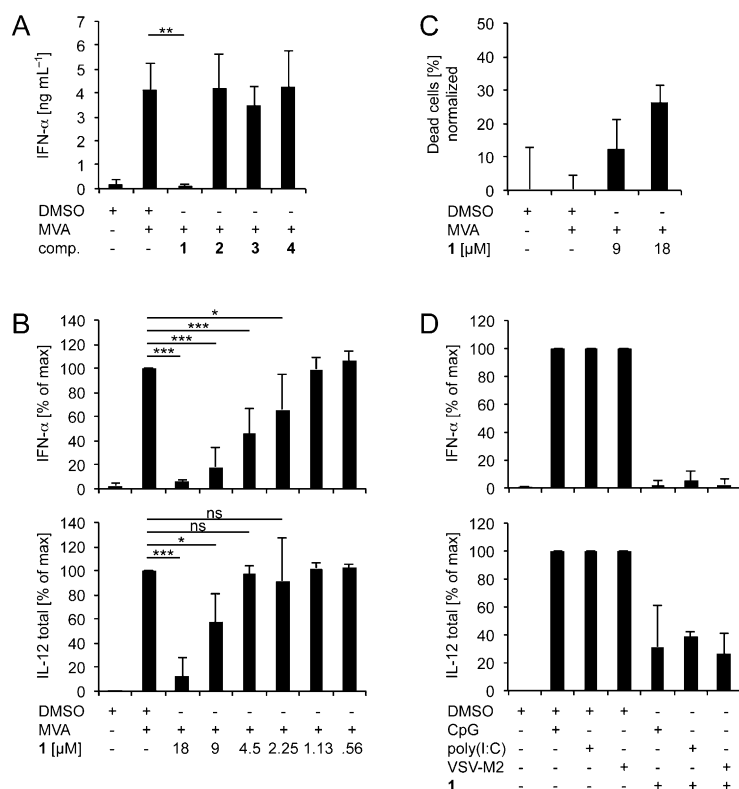


Figure 2. Compound **1** specifically inhibits MVA-induced IFN-α responses by BM-pDCs. A) BM-pDCs were infected with MVA at a multiplicity of infection of 1 (*moi* 1) and treated with compounds (18 μM; dissolved in DMSO). Control cells were treated with DMSO only (corresponding concentration) or were infected with MVA at *moi* 1, additionally. At 24 h after treatment, the supernatants were analyzed for IFN-α by ELISA (*n* = 3). B) BM-pDCs were infected with MVA at *moi* 1 and treated with compound **1** (in DMSO) at the indicated concentrations. Control cells were treated with DMSO only (highest concentration) or were infected with MVA at *moi* 1, additionally. At 24 h after treatment, the supernatants were analyzed for IFN-α or total IL-12 (detecting IL-12p70 and p40) by ELISA. Values shown are normalized to MVA-induced IFN-α or total IL-12 production (*n* = 5). C) BM-pDCs were infected with MVA at *moi* 1 and treated with compound **1** (dissolved in DMSO) at the indicated concentrations. Control cells were treated with DMSO only (highest concentration) or were infected with MVA at *moi* 1, additionally. At 18 h after treatment, cells were harvested, stained with propidium iodide, and analyzed by FACS. Percentages shown are normalized to MVA-induced cell death (*n* = 4). D) BM-pDCs were stimulated with CpG2216 at 5 μg mL⁻¹, transfected with 2 μg poly(I:C) or infected with VSV-M2 at *moi* 1. Where indicated, cells were additionally treated with compound **1** (9 μM). Control cells were treated with DMSO only (corresponding concentration) or were infected with MVA at *moi* 1, additionally. At 24 h after treatment, the supernatants were analyzed for IFN-α or total IL-12 (detecting IL-12p70 and p40) by an ELISA method. Values shown are normalized to CpG2216-, poly(I:C)-, or VSV-M2-induced IFN-α production (*n* = 3). Error bars indicate standard deviations. ns: not significant; *: *p* < 0.05 ≥ 0.01; **: *p* < 0.01 ≥ 0.001; ***: *p* < 0.001 (Dunnett test or pairwise Bonferroni permutation test).

STD spectra (Figure 3F) it is evident that no saturation transfer occurs between IFN-α and the glycoside. When compound **1** was added to the mixture of methyl-β-D-glucopyranoside and IFN-α (Figure 3G) and the STD experiment was repeated, saturation transfer from IFN-α to compound **1** was again observed (Figure 3H). Based on these results we conclude that compound **1** exerts immunosuppressive activity by the direct interaction with IFN-α.

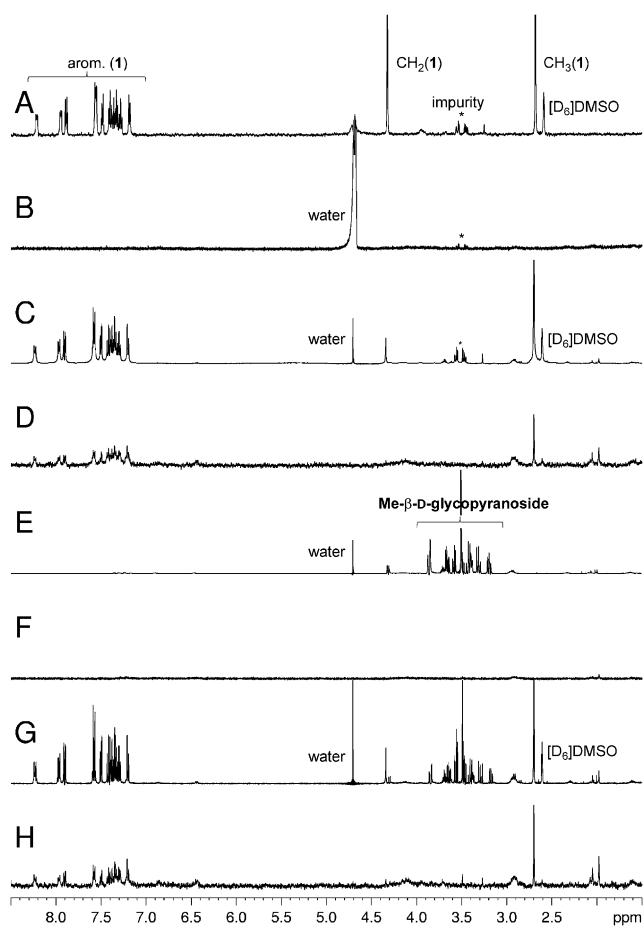


Figure 3. STD NMR experiment revealing the direct interaction between compound **1** and IFN-α. A) ¹H NMR spectrum of the ligand, compound **1** (1 mM). B) ¹H NMR spectrum of human IFN-α (40 μM, CYT-204, Prospecc Ltd, Ness-Ziona, Israel). C) Off-resonance reference NMR spectrum of compound **1** (1 mM) in the presence of IFN-α (40 μM). D) STD NMR spectrum of compound **1** (1 mM) in the presence of IFN-α (40 μM). E) Off-resonance reference NMR spectrum of methyl-β-D-glucopyranoside (1 mM). F) STD NMR spectrum of methyl-β-D-glucopyranoside (1 mM). G) Off-resonance reference NMR spectrum of compound **1** (1 mM) together with methyl-β-D-glucopyranoside (1 mM) in the presence of IFN-α (40 μM). H) STD NMR spectrum of compound **1** (1 mM) together with methyl-β-D-glucopyranoside (1 mM) in the presence of IFN-α (40 μM). In (A), (B), and (C) a minor impurity was observed at 3.52 ppm in addition to residual water: the expected signals, and residual protons of deuterated solvent ([D₆]DMSO). The impurity is not present in the STD spectrum (Figure 3D) indicating that it does not interact with IFN-α. Figure 3D clearly shows saturation transfer from IFN-α to the aromatic protons of compound **1** (7.0–8.5 ppm) and to the methyl group at 2.7 ppm, while saturation transfer to the CH₂ group (4.3 ppm) seems to be rather weak. The spectra in (E) and (F) demonstrate that no saturation transfer occurs between IFN-α and methyl-β-D-glucopyranoside. The spectrum in (H) presents the observed saturation transfer from IFN-α to the aromatic protons of compound **1** (7.0–8.5 ppm), and to the methyl group (at 2.7 ppm, in (D)) in the mixture between compound **1** and methyl-β-D-glucopyranoside with IFN-α, indicating the selective saturation transfer to the binding ligand.

Using SPR measurements^[25] we determined a low micromolar value of the dissociation constant (*K*_d = 4 μM) for the interaction of compound **1** with human IFN-α (Figure S1 in

the Supporting Information). Dynamic light scattering did not indicate any detectable compound aggregation that might have led to measurement artifacts. Its low molecular weight (279 Da) qualifies the inhibitor for chemical optimization to further increase ligand efficiency and enter lead-structure development.^[26]

Our results confirm that predictions based on protein–protein interfaces and “hot spots” can serve as a solid basis for drug-discovery projects,^[27] thus making it possible to systematically address the pharmacologically highly relevant, but often challenging inhibition of protein–protein interactions.

Note added in proof: An X-ray structure of the (IFN)–(IFNAR2-EC) complex (PDB ID: 3s9d^[28]) was published after completion of our study, confirming the importance of the hydrophobic area containing Phe²⁷ and Leu³⁰ as well as the key interaction of Arg¹⁴⁹, which forms a salt bridge to Glu⁷⁷ upon complex formation with IFNAR2-EC.

Received: August 20, 2011

Published online: November 16, 2011

Keywords: bioinformatics · drug design · interferon · protein–protein interactions · virtual screening

- [1] L. Malmgaard, *J. Interferon Cytokine Res.* **2004**, *24*, 439–454.
- [2] A. Le Bon, D. F. Tough, *Cytokine Growth Factor Rev.* **2008**, *19*, 33–40.
- [3] M. Swiecki, M. Colonna, *Immunol. Rev.* **2010**, *234*, 142–162.
- [4] K. E. Mogensen, M. Lewerenz, J. Reboul, G. Lutfalla, G. Uzé, *J. Interferon Cytokine Res.* **1999**, *19*, 1069–1098.
- [5] D. Finke, M. L. Eloranta, L. Rönnblom, *Autoimmunity* **2009**, *42*, 349–352.
- [6] L. E. Wilson, D. Widman, S. H. Dikman, P. D. Gorevic, *Semin. Arthritis Rheum.* **2002**, *32*, 163–173.
- [7] a) D. Hober, P. Sauter, *Nat. Rev. Endocrinol.* **2010**, *6*, 279–289; b) C. Selmi, A. Lleo, M. Zuin, M. Podda, L. Rossaro, M. E. Gershwin, *Curr. Opin. Invest. Drugs* **2006**, *7*, 451–456.
- [8] a) A. Dömling, *Curr. Opin. Chem. Biol.* **2008**, *12*, 281–291; b) T. Berg, *Curr. Opin. Drug Discov. Devel.* **2008**, *11*, 666–674; c) D. González-Ruiz, H. Gohlke, *Curr. Med. Chem.* **2006**, *13*, 2607–2625.
- [9] W. Klaus, B. Gsell, A. M. Labhardt, B. Wipf, H. Senn, *J. Mol. Biol.* **1997**, *274*, 661–675.
- [10] S. R. Quadt-Akabayov, J. H. Chill, R. Levy, N. Kessler, J. Anglister, *Protein Sci.* **2006**, *15*, 2656–2668.
- [11] H. M. Berman, J. Westbrook, Z. Feng, G. Gilliland, T. N. Bhat, H. Weissig, I. N. Shindyalov, P. E. Bourne, *Nucleic Acids Res.* **2000**, *28*, 235–242.
- [12] F. P. Davis, A. Sali, *PLoS Comput. Biol.* **2010**, *6*, e1000668.
- [13] R. Najmanovich, J. Kuttner, V. Sobolev, M. Edelman, *Proteins Struct. Funct. Genet.* **2000**, *39*, 261–268.
- [14] M. Weisel, E. Proschak, G. Schneider, *Chem. Cent. J.* **2007**, *1*, 7.
- [15] T. Geppert, B. Hoy, S. Wessler, G. Schneider, *Chem. Biol.* **2011**, *18*, 344–353.
- [16] J. Piehler, G. Schreiber, *J. Mol. Biol.* **1999**, *289*, 57–67.
- [17] J. Piehler, G. Schreiber, *J. Mol. Biol.* **1999**, *294*, 223–237.
- [18] a) M. Löwer, T. Geppert, P. Schneider, B. Hoy, S. Wessler, G. Schneider, *PLoS One* **2011**, *6*, e17986; b) A. Klenner, M. Hartenfeller, P. Schneider, G. Schneider, *Drug Discovery Today Technol.* **2010**, *7*, e237–e244.
- [19] G. Jones, P. Willett, R. C. Glen, *J. Mol. Biol.* **1995**, *245*, 43–53.
- [20] Z. Waibler, M. Anzaghe, H. Ludwig, S. Akira, S. Weiss, G. Sutter, U. Kalinke, *J. Virol.* **2007**, *81*, 12102–12110.
- [21] Z. Waibler, M. Anzaghe, A. Konur, S. Akira, W. Müller, U. Kalinke, *Eur. J. Immunol.* **2008**, *38*, 3127–3137.
- [22] G. Kochs, S. Bauer, C. Vogt, T. Frenz, J. Tschopp, U. Kalinke, Z. Waibler, *J. Virol.* **2010**, *84*, 12344–12350.
- [23] Z. Waibler, C. N. Detje, J. C. Bell, U. Kalinke, *Immunobiology* **2008**, *212*, 887–894.
- [24] M. Mayer, B. Meyer, *Angew. Chem.* **1999**, *111*, 1902–1906; *Angew. Chem. Int. Ed.* **1999**, *38*, 1784–1788.
- [25] a) H. Raether, E. Kretschmann, *Z. Naturforsch. A* **1968**, *23*, 2135–2136; b) *Surface Plasmon Resonance* (Eds.: N. J. de Mol, M. J. E. Fischer), Humana Press, New York, **2010**.
- [26] a) A. L. Hopkins, C. R. Groom, A. Alex, *Drug Discovery Today* **2004**, *9*, 430–431; b) C. W. Murray, T. L. Blundell, *Curr. Opin. Struct. Biol.* **2010**, *20*, 497–507; c) E. Feyfant, J. B. Cross, K. Paris, D. H. Tsao, *Methods Mol. Biol.* **2011**, *685*, 241–252; d) M. Hartenfeller, G. Schneider, *Wiley Interdiscip. Rev. Comput. Mol. Sci.* **2011**, *1*, 742–759.
- [27] a) N. Tuncbag, O. Keskin, A. Gursoy, *Nucleic Acids Res.* **2010**, *38*, W402–W406; b) L. M. Meireles, A. S. Dömling, C. J. Camacho, *Nucleic Acids Res.* **2010**, *38*, W407–W411; c) A. Shulman-Peleg, M. Shatsky, R. Nussinov, H. J. Wolfson, *BMC Biol.* **2007**, *5*, 43.
- [28] C. Thomas, I. Moraga, D. Levin, P. O. Krutzik, Y. Podoplelova, A. Trejo, C. Lee, G. Yarden, S. E. Vleck, J. S. Glenn, G. P. Nolan, J. Piehler, G. Schreiber, K. C. Garcia, *Cell* **2011**, *146*, 621–632.